DYNAMIC STABILITY OF PLANING SHIPS

S L Toxopeus, Delft University of Technology, The Netherlands
J A Keuning, Delft University of Technology, The Netherlands
J P Hooft, MARIN, Wageningen, The Netherlands

SUMMARY

At present, most of the dynamic research on planing ships has been directed towards analysing the ship's motions in either the 3-DOF (Degrees Of Freedom) mode in the longitudinal vertical plane or in the 3-DOF or 4-DOF mode in the lateral vertical plane.

For this reason Delft University of Technology and MARIN have started the set-up of describing the dynamic behaviour of planing ships in a 6-DOF mathematical model. This research program consisted first of all in developing a 6-DOF computer simulation program in the time domain. Such a simulation program is to be used to predict the response of these type of vessels to disturbances during high speed sailing.

For describing the behaviour of planing ships in still water static tests have been executed with two planing hull forms in the towing tank of Delft University of Technology. The test program consisted of measuring three force- and three moment components as a function of the pitch, rise (draught), roll, drift and speed of the model.

At a next stage a model test program is anticipated to determine the added mass and damping components of these two hull forms and also the rudder forces. In the meantime the program is in operation while using empirically estimated values for these quantities.

In this paper the set-up of the mathematical model will be presented. Also a discussion will be given about the use of these static contributions in a time domain simulation to model the behaviour of the ship.

AUTHORS' BIOGRAPHIES

Mr S L Toxopeus graduated from the Delft University of Technology in 1996. He is currently employed as project manager at the Maritime Research Institute of the Netherlands in Wageningen.

Dr J A Keuning graduated from the Delft University of Technology in 1977 and obtained his doctorate at Delft University of Technology in 1994. He is employed as a lecturer at the Ship Hydromechanics Department of Delft University of Technology, his main subject being the dynamics of advanced naval vehicles, including sailing yachts.

Dr J P Hooft graduated from the Delft University of Technology in 1962 and obtained his doctorate at Delft University of Technology in 1970. He has been employed at MARIN since 1962. He is currently senior project manager involved in developing mathematical models for simulating the behaviour of various kinds of marine structures.

1. INTRODUCTION

The motions of planing craft have been the subject of many research projects during the last few decades. The dynamic research was largely directed towards analysing the motions of the ship in either the longitudinal vertical plane for three degrees of freedom, see e.g. [13], [19], or in the four-DOF mode in the lateral vertical plane or horizontal plane [9], [14]. Reviewing the literature about dynamic stability of high speed craft, it appears that a mathematical model with six degrees of freedom does not exist.

At present it is thought that incorporating all six degrees of freedom into the mathematical models becomes increasingly important. Instabilities have been reported in both longitudinal and lateral directions with motions ranging from rapid loss of running trim, progressive heeling, broaching or a sudden combined roll-yaw motion, possibly resulting in crew injury or craft loss (Refs. 14, 20 and 21). Most instabilities are suspected to originate from coupling between the six degrees of motions. For example, large bow-down trim angles will most likely result in transverse instability: yaw motions. For reliable prediction of the dynamic stability and manoeuvrability of planing craft, all six degrees of freedom have to be accounted for.

For describing the behaviour of planing ships in still water, static captive model tests have been executed with two planing hull forms in the towing tank at Delft University of Technology, see Reference [17]. The test program consisted of measuring three force and three moment components as a function of the pitch, rise (draught), roll, drift and speed of the models. At a future stage a model test program is anticipated to determine the added mass and damping forces of these planing hull forms and also the rudder and propeller forces acting on the models. At present, the computer program is in operation while using empirically estimated values for these quantities.

In this paper, the set-up of the preliminary non-linear mathematical model for six degrees of freedom based on

the data obtained from the model experiments will be described. This mathematical model has been incorporated in a time-domain computer simulation program in order to predict the dynamic stability and manoeuvrability of a planing ship, see Reference [16]. The results of some simulations performed will be included and discussed. Also, recommendations will be made for further study, to increase the accuracy of the mathematical model.

2.   COORDINATE SYSTEM

The coordinate systems used in this study are cartesian coordinate systems. One coordinate system is the ship-fixed coordinate system, with the x-axis pointing forward perpendicular to the baseline of the ship and the z-axis downward. The y-axis is pointed to starboard. The origin is at the intersection of frame 0 and the baseline of the model.

The x-y-plane of the earth-fixed coordinate system coincides with the undisturbed water surface, the z-axis is pointed downward.

Rotations in both coordinate systems are positive if clockwise, looking in positive direction. The roll angle ϕ, the pitch angle θ and the yaw angle ψ are rotations around the ship-fixed x, y and z axis respectively. The drift angle is used to define the non-dimensional lateral velocity component:

$$\beta = \psi - \arctan\left(\frac{v_\bullet}{u_\bullet}\right)$$

with u being the longitudinal velocity component.

3.   MODEL TESTS

3.1   MODEL PARTICULARS

The models used for this study are Model 233 and Model 277 of Delft University of Technology. Model 277 is based on the Clement and Blount [1] 62 series with a deadrise of 25 degrees. Keuning [6] performed seakeeping tests with this model. Model 233 is used by Keuning et al [8] during experiments with models with warped bottoms. The main particulars are stated in the table below:

	Symbol	Model 233	Model 277
Type		Deadrise 25°	Twisted bottom
Length	L	1.50m	1.50m
Max. beam at chine	B_{max}	0.367m	0.367m
Projected area	A_P	0.450m²	0.4589m²
Centre of planing area forward of ord 0	C_{AP}	48.8%L	48.8%L
Length/Beam ratio	L/B	4.09	4.09
Mass model incl. transducer	m	9.45kg	6.67kg
Longitudinal centre of reference	$LCOR$	0.726m	0.726m
Vertical centre of reference	$VCOR$	0.080m	0.080m

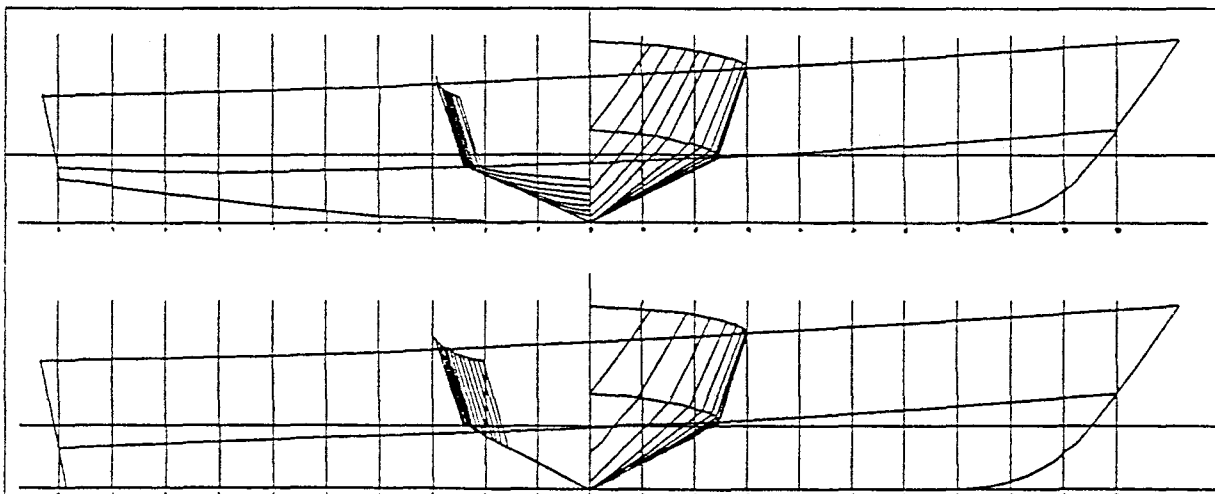*In Figure 1 the body plans of both models are included*

Figure 1   Body plans of Model 233 (above) and Model 277 (below)

3.2 TEST PROGRAM

In the present study some static captive tests have been performed with both models during which the forces and moments in the six degrees of freedom were measured. These tests will only provide a limited amount of information about the hydrodynamics of planing ships. Therefore in further studies additional tests will be performed to determine the remaining hydrodynamic characteristics.

The following variables have been tested:

Speed U:

the speed has great influence on the position of the ship relative to the free water surface. A change in speed will result in a change of trim and rise. The model was tested at the speeds of: $U_1 = 2.0ms^{-1}$, $U_2 = 3.0ms^{-1}$ and $U_3 = 4.0ms^{-1}$.

Pitch θ:

For planing ships, the pitch varies due to speed variations and has great effect on the lift and drag and on the dynamic stability. A combination of low pitch angle and roll or drift can result in large yaw moments. The model was tested at the pitch angles of: $\theta_1 = -2^\circ$, $\theta_2 = 3^\circ$ and $\theta_3 = 5^\circ$.

Drift β:

To study the effect of drift, the model was tested at three drift angles of: $\beta_1 = 0^\circ$, $\beta_2 = 5^\circ$ and $\beta_3 = 10^\circ$.

Roll ϕ:

Also the influence of the roll angle has been determined as it affects the transverse and course stability of the planing ship. The model was tested at four roll angles of: $\phi_1 = 0^\circ$, $\phi_2 = 5^\circ$, $\phi_3 = 10^\circ$ and $\phi_4 = -5^\circ$. The negative roll angle was only tested with Model 277, to study the effect of symmetry.

Rise of COR z:

The rise of the centre of reference z has great influence on the behaviour of planing ships. When the ship accelerates from zero to full speed, first the ship sinks more into the water, while at higher speed the lift force pushes the ship out of the water. Assuming the design draughts of both models were $T = 0.080m$, a negative rise of $z = -5mm$ and a positive rise of $15mm$ were chosen, corresponding to draughts of $T = 0.085mm$ and $T = 0.065mm$ respectively.

The ranges of the variables were chosen after examining previous results of model experiments with Model 233 [8] and Model 277 [6].

Some combinations of the variables were skipped during the experiments due to expected problems with spray. The total number of test runs was 304.

3.3 EXPERIMENTAL SET-UP

Two six-component transducers were fixed into the models, evenly spaced around the centre of reference. Adding the components of the transducers, three forces and three moments about the centre of reference could be found.

The measurement of the forces was divided in two parts: a velocity independent part at speed $U = 0ms^{-1}$ and a velocity dependent part, obtained by measuring the change in forces due to the towing speed. Adding the two components yields the total force acting on the hull during the run.

The forces and moments acting on the hull in the centre of reference COR as a function of speed, drift, trim, roll and rise have been published in Reference [17]. The forces and moments acting in any arbitrary centre of gravity CG are found after transforming the values from the COR to the CG.

4. MATHEMATICAL MODEL

4.1 FORCES AND MOMENTS BASED ON EXPERIMENTAL DATA

Using the data obtained from the model experiments in tabular form in the computer program poses two difficulties. First, interpolating in a five dimensional parameter space is rather complex, especially since certain combinations of variables were not used during the experiments. Secondly, because of the six degrees of freedom, the amount of memory needed during the simulation would be rather high. It was therefore decided to describe the data by mathematical formulations derived from regression analysis.

The hydrodynamic forces acting on the hull comprise of linear as well as non-linear components. The basic structure of the analysis of the mathematical model of the hydrodynamic forces is described in full detail in Reference [16].

It must be noted that the mathematical model found in this study is only valid to describe the forces and moments acting on the two ship models, Model 233 and Model 277, because the coefficients in the mathematical descriptions are not presented in non-dimensional form. In further studies, the scale effects should be examined to be able to predict stability and manoeuvring characteristics for full-sized planing ships.

4.2 DAMPING FORCES

It was desired to run the computer simulation program without having determined the damping of most of the motion components. Therefore use has been made of some rough values of the damping coefficients in the roll and pitch motions.

In future studies additional tests will be conducted to determine the damping of planing hulls at a higher

accuracy. In this aspect it is thought that only roll and pitch decay tests will already provide more information about the damping factors.

For the present research, the damping coefficients in the x, y and z direction are supposed to be incorporated in the mathematical model. It is also assumed that the couple terms are comparatively small and can therefore be neglected. The remaining damping coefficients $K(p)$, $M(q)$ and $N(r)$ remain to be determined in more detail, especially as a dependency on the speed.

4.2(a) Roll damping

For planing ships with deadrise and hard chines, damping of roll motion is relatively high, because of the immersion of the planing area at roll angles. Therefore the non-dimensional damping factor κ_ϕ defined as:

$$\kappa_\phi = \frac{v}{\omega} = \frac{b}{2\sqrt{(I_{xx}+M_{pp})\cdot c}}$$

is assumed to have a relatively large value. Using the following equation yields the damping coefficient b, when κ_ϕ and the time-dependent I_{xx}, M_{pp} and c are known, see also Rutgersson and Ottosson [14]:

$$b = 2\cdot\kappa_\phi\sqrt{(I_{xx}+M_{pp})\cdot c}$$

The spring coefficient c is taken from the mathematical model of the roll moment and depends on the position and speed of the ship, while the added mass coefficient M_{pp} is determined below.

In the present study, κ_ϕ has been varied in the simulation program in order to ascertain the influence of the roll damping coefficient. From experimental observations with free running ships sailing a straight course at high speed at an initially non-zero roll angle, it was found that the decay of the roll would occur during a limited number of oscillations until a stable situation is reached. The value of κ_ϕ should therefore be chosen such that also during the simulation the number of oscillations is found to be small (approximately one or two). It is expected that κ_ϕ is speed dependent and may therefore vary in time as a consequence of the change of speed.

The damping moment for roll is now: $K_{damp}=K_p\cdot p=-b\cdot p$

4.2(b) Pitch damping

In this study, the pitch damping will be modelled similar to the roll damping. The following equation is used for determining the time-dependent pitch damping:

$$b = 2\cdot\kappa_\theta\sqrt{(I_{yy}+M_{qq})\cdot c}$$

The damping moment for pitch is now: $M_{damp}=M_q\cdot q=-b\cdot q$

Similar to the formulation of K_p, the damping coefficient M_{uq} is thought to be implemented in M_q through the speed dependency in κ_θ.

4.2(c) Yaw damping

Inoue [4] and Hooft [2] give an empirical expression for the damping coefficient of the yaw motion. Based on these expressions the following equation is used in the simulation program:

$$N_{ur}=-\frac{\pi}{2}\rho L^2 T^2 (0.25+0.039\frac{B}{T}-0.56\frac{B}{L})\cdot(1+0.3\frac{L\tan\theta}{T})$$

where B and T are the time-dependent maximum beam and draught of the ship. In this study, it is assumed that the non-linear damping term $N_{r|r|}$ is small compared to N_{ur} and can therefore be neglected.

The damping moment for yaw is now: $N_{damp}=N_{ur}\cdot u\cdot r$

4.3 PROPELLER FORCES

Various methods exist to predict the thrust of the propeller as a function of the propeller rate of turning and the ship's longitudinal speed. Also approximations exist to take into account the effect of the lateral motions of the propeller. Often, however, the exact dimensions of the propeller are not yet determined in the initial design stage.

Therefore a simplified description of the propeller effect is used in the simulation program which is assumed to be acceptable when the propeller RPM are not affected by the motions of the ship. It should be noted that these formulae assume that the axis of the propeller shaft is parallel to the ship-fixed x-axis.

For this study one determines the propeller thrust X_{prop} from:

$$X_{prop}=\rho D_p^4 K_T n^2$$

in which D_p is the diameter of the propeller and n the number of revolutions per second. The thrust coefficient K_T is described by:

$$K_T=K_{T0}+K_{T1}\cdot J+K_{T2}\cdot J^2+K_{T3}\cdot J^3$$

in which the advance ratio J is defined by: $J=\dfrac{u_p\cdot(1-w_p)}{n\cdot D_p}$

where u_p is the propeller inflow velocity and w_p is the propeller wake fraction. The coefficients K_{Ti} have to be determined otherwise and are required as input to the simulation program.

Using the distances between the propeller and CG, $y_{prop}-y_g$ and $z_{prop}-z_g$, the pitch and yaw moment induced by the propeller thrust are calculated with:

$$M_{prop}=(z_{prop}-z_G)\cdot X_{prop}$$
$$N_{prop}=-(y_{prop}-y_G)\cdot X_{prop}$$

The current formulae do not take the propeller torque into account to induce a roll moment.

4.4   RUDDER FORCES

The formulation of the rudder forces is based on Inoue [5] and Hooft [2], [3]. The rough approximations are suitable for the preliminary design process, when the actual rudder dimensions are not determined in detail. It is assumed that the velocities around the rudder are high and that flow separation does not occur. This last assumption should be re-evaluated in future studies to increase the accuracy of the prediction of the rudder forces. For this preliminary study, added mass and damping of the rudders are neglected. To increase the accuracy, these factors are to be included in future studies.
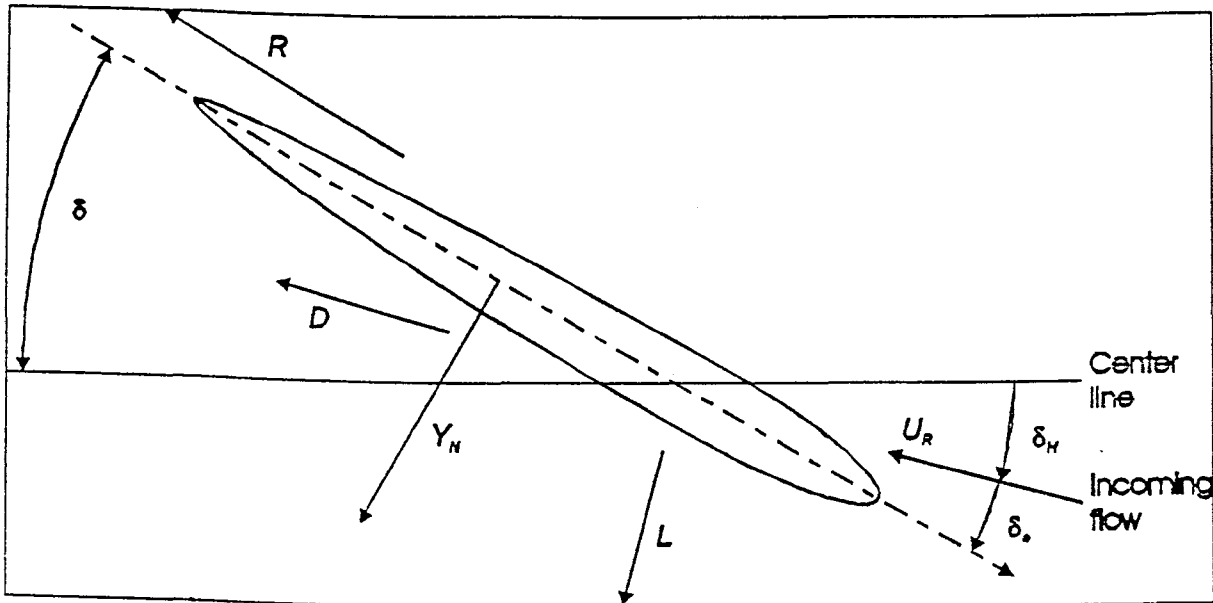

Figure 2 Forces acting on the rudder

To determine the forces on the rudder, as defined in Figure 2, the local effective rudder inflow velocity and the apparent angle of incidence have to be calculated.

The local rudder inflow velocity for a rudder with average height h_r, average chord length c_r, lateral rudder area A_r and effective aspect ratio A_e, is approximated by:

$$u_r = u \cdot (1 - \dot{w}_p) + C_{Du} \cdot \Delta u_p$$

$$v_r = C_{ab} \cdot (v \cos \phi_F + w \sin \phi_F) - C_{dr} \sqrt{x_r^2 + y_r^2} \, r + C_{dr} \sqrt{x_r^2 + z_r^2} \, q$$

$$U_{rud} = \sqrt{u_r^2 + v_r^2}$$

where

$$C_{Du} = \; 0.7 \frac{D_p}{h_r} \; [3] \; \text{or} \; 0.9 \frac{D_p}{h_r} \; [2] \; \text{effectiveness of velocity increment}$$

$$\Delta u_p = \sqrt{u_p^2 + \frac{8 \cdot X_{prop}}{\rho \pi D_p^2}} - u_p \quad \text{velocity increment}$$

$C_{ab} \approx 0.7$ flow straightening factor

$C_{dr} \approx 1.0$

ϕ_f angle between rudder and vertical plane

x_r, y_r, z_r position of rudder relative to CG

The effective angle of incidence of the flow to the rudder follows from: $\delta_e = \delta - \delta_H$ where $\delta_H = \arctan \frac{v_r}{u_r}$.

The lateral rudder force can now be determined, using the above equations, with:

$$L = \frac{1}{2} \rho A_r C_{L\delta} U_{rud}^2 \sin \delta_e$$

where

$$C_{L\delta} \approx \frac{6.13 \cdot A_e}{A_e + 2.25} \; [2] \; \text{rudder lift coefficient}$$

The lift induced drag in the direction of the rudder inflow is described by:

$$D = \frac{1}{2} \rho A_r C_{Di} U_{rud}^2 \sin^2 \delta_e$$

where

$$C_{Di} = \frac{C_{L\delta}^2}{\pi A_e} \; \text{rudder lift induced drag coefficient}$$

The friction resistance of the rudder due to the friction drag of the rudder is formulated as:

5

$$R = \frac{1}{2}\rho S_{wr} C_{TR}\left(U_{rud}\cos\delta_e\right)^2$$

where

S_{wr} $\approx 2 \cdot A_r$ rudder wetted area

C_{TR} ≈ 0.017 [3] high-lift rudder friction coefficient

       ≈ 0.007 [3] NACA profile friction coefficient

The normal force on the rudder due to the lateral drag coefficient $C_N \approx 1.8$ is:

$$Y_N = \frac{1}{2}\rho A_r C_N U_{rud}\sin\delta_e |U_{rud}\sin\delta_e|$$

Due to these rudder forces, one finds the following descriptions for the rudder induced forces on the ship:

$$X_{rud} = -R\cos\delta - D\cos\delta_H - Y_N\sin\delta - L\sin\delta_H$$
$$Y_{rud} = (-R\sin\delta - D\sin\delta_H + Y_N\cos\delta + (1+a_h)L\cos\delta_H)\cdot\cos\phi_F$$
$$Z_{rud} = (-R\sin\delta - D\sin\delta_H + Y_N\cos\delta + (1+a_h)L\cos\delta_H)\cdot\sin\phi_F$$
$$K_{rud} = -Y_{rud}\cdot z_r + Z_{rud}\cdot y_r$$
$$M_{rud} = X_{rud}\cdot z_r + Z_{rud}\cdot x_r$$
$$N_{rud} = -X_{rud}\cdot y_r + \left(\left(Y_N\cos\delta - R\sin\delta - D\sin\delta_H\right)\cdot x_r + (x_r + a_h\cdot x_h)L\cos\delta_H\right)\cos\phi_F$$

where

a_h $\approx 0.672\cdot C_B - 0.153$ [2]

       increase of rudder efficiency due to induced force on ship's hull

x_h $\approx 0.9\cdot x_r$ distance of induced hull force to centre of gravity

4.5 TOTAL EXCITATION FORCES

In this preliminary study, the forces and moments dealt with in the previous sections are supposed to be sufficient to predict the forces and moments acting on the tested planing hull forms sailing in calm water. To predict the behaviour of a vessel in all weather and sea conditions, descriptions to model the influence of waves, wind and current on the ship have to be incorporated.

It is generally known that the wave forces have a large influence on the behaviour of the ship, but the influence of wind can also be large. A strong side wind can induce large roll angles, changing the hydrodynamic forces and moments considerably. Strong wind gusts can result in coupled roll-yaw motions, possibly resulting in broaching or capsizing.

The total excitation forces and moments about the centre of reference in ship-fixed directions are found by adding all force components:

$$\Sigma F = F_{exc} = F_{grav} + F_{hull} + F_{damp} + F_{prop} + F_{rud}$$

This equation is used for calculating the accelerations of the ship.

4.6 ADDED MASS

4.6(a) Considerations

In this section, the description of the added mass of the planing ship models will be formulated based on descriptions from strip theory. The symbol used for the added mass of a strip at position x in direction i for an acceleration in direction k is:

$$m_{ik}(x) \quad \text{with} \quad i,k = 1\ldots 6 \quad \text{or} \quad x,y,z,\phi,\theta,\psi$$

In Reference [10], Papanikolaou formulated the added mass per unit length for sway, heave and roll of a floating cylinder using potential theory. It can be shown that:

$$m_{ik}(x) = m_{ki}(x)$$

and on grounds of symmetry:

$$m_{ik}(x) = 0 \quad \text{for } i + k \text{ odd}$$

With these considerations, the added mass matrix for a strip at position x looks like:

$$\begin{bmatrix} m_{xx} & 0 & m_{xz} & 0 & m_{x\theta} & 0 \\ 0 & m_{yy} & 0 & m_{y\phi} & 0 & m_{y\psi} \\ m_{xz} & 0 & m_{zz} & 0 & m_{z\theta} & 0 \\ 0 & m_{y\phi} & 0 & m_{\phi\phi} & 0 & m_{\phi\psi} \\ m_{x\theta} & 0 & m_{z\theta} & 0 & m_{\theta\theta} & 0 \\ 0 & m_{y\psi} & 0 & m_{\phi\psi} & 0 & m_{\psi\psi} \end{bmatrix}$$

In most reports, the added mass of a section with half beam b is taken proportional to the mass of a semi-circle with radius b and specific mass ρ: $m_{ij} = \frac{1}{2}\pi b^2 \rho \cdot f_1(\beta, T,\ldots)$.

When the chines of the ship are not immersed, the draught T of the ship is a measure for the half beam b, therefore one can also write: $m_{ij} = \frac{1}{2}\pi T^2 \rho \cdot f_2(\beta, T,\ldots)$.

This factor can also be seen in the formulations for the added mass in this paper.

4.6(b) Added mass for x-direction

Because the values of m_{xz} and $m_{x\theta}$ are presumably small compared to m_{xx}, these added masses are taken to be zero in the present study. In future studies, these components can be assigned non-zero values if desired to increase accuracy.

For this study, the total added mass M_{xx} can be approximated by

$$M_{xx} = \frac{\pi\rho T_{max}^2 B_{max}}{2}\cdot C_{mx}$$

where C_{mx} is taken as: $C_{mx} = 0.8$. The parameters T_{max} and B_{max} are the time-dependent instantaneous maximum draught and breadth at the still water line of the ship.

4.6(c) Added mass for y-direction

Papanikolaou gives in his report tables to determine the added mass in y-direction for variable excitation frequencies and breadth to draught ratios. In the present study, the values for $\omega = 0\ s^{-1}$ should be used, because the equations of motions are solved for a quasi-static state of the ship.

Diagram 4 from [10] gives the non-dimensional added mass coefficient m_{yy}' of a section as a function of the beam to draught ratio. The values in this figure for zero oscillation frequency will be approximated in this study using the following function:

$$m_{yy}'=m_{yy0}+m_{yy1}\left(\frac{B}{T}\right)+m_{yy2}\left(\frac{B}{T}\right)^2+m_{yy3}\left(\frac{B}{T}\right)^3$$

The coefficients m_{yyi} are determined by performing regression analysis. This results in the following coefficients:

$m_{yy0}=1.0274 \quad m_{yy1}=-0.1947 \quad m_{yy2}=0.0358 \quad m_{yy3}=-0.0023$

Care should be taken using this formula for high $\left(\frac{B}{T}\right)$ values (greater than approximately 5). Because of the regression model, extrapolating will yield unrealistic results.

The added mass in y-direction per unit length for a section with draught T can now be derived with:

$$m_{yy}=\frac{\pi\rho T^2}{2}\cdot m_{yy}'$$

When m_{yy} is known, the following added masses can be calculated:

$$M_{yy}=\int_L m_{yy}\ dx \quad M_{y\psi}=M_{\psi y}=\int_L m_{yy}\cdot x\ dx \quad M_{\psi\psi}=\int_L m_{yy}\cdot x^2\ dx$$

Papanikolaou also gave a relation between the added masses $m_{y\phi}$ and m_{yy} by plotting the virtual arm $h_{y\phi}=\frac{m_{y\phi}}{m_{yy}\cdot T}$.

These values will be approximated using $m_{y\phi}=m_{yy}\cdot T\cdot h_{y\phi}$ and

$$h_{y\phi}=h_{y\phi0}+h_{y\phi1}\left(\frac{B}{T}\right)+h_{y\phi2}\left(\frac{B}{T}\right)^2+h_{y\phi3}\left(\frac{B}{T}\right)^3$$

Performing regression analysis yields the following coefficients for the virtual arm:

$h_{y\phi0}=0.4472 \quad h_{y\phi1}=-0.0218 \quad h_{y\phi2}=-0.1349 \quad h_{y\phi3}=-0.0007$

The added mass $M_{y\phi}$ can be calculated with:

$$M_{y\phi}=\int_L m_{y\phi}\ dx.$$

4.6(d) Added mass for z-direction

The added mass for an acceleration in z-direction is described by Payne [11] and Quadvlieg [13]. Both reports give the following description for the added mass per unit length for a section with deadrise angle β and draught T as:

$$m_{zz}=\frac{\pi\rho T^2}{2\cdot\tan^2\beta}\cdot f(\beta)$$

The function $f(\beta)$ gives the quotient of the added mass for a prism and the added mass for a flat plate. According to Payne, $f(\beta)$, with β in radians, is given by $f(\beta)=1-\frac{\beta}{\pi}$ while Quadvlieg gives: $f(\beta)=1-\frac{2\cdot\beta}{\pi}$. For zero deadrise, a flat plate, both deadrise functions yield the same value, i.e. $f(0) = 1$. However, for a deadrise of $\frac{\pi}{2}$, the function by Payne gives $f(\frac{\pi}{2})=\frac{1}{2}$, while the function of Quadvlieg results in $f(\frac{\pi}{2})=0$.

In this study, it is decided to use the description by Quadvlieg in the simulation program. Further study should examine the added mass in more detail to determine which formulation yields more realistic results. Recent work by Payne [12] gives suggestions on improvements in the determination of the added mass.

This added mass per unit length m_{zz} can now be used to calculate the following added masses:

$$M_{zz}=\int_L m_{zz}\ dx \quad M_{z\theta}=M_{\theta z}=\int_L m_{zz}\cdot x\ dx \quad M_{\theta\theta}=\int_L m_{zz}\cdot x^2\ dx$$

4.6(e) Added mass for φ-direction

The hydrodynamic mass in φ-direction, depending on the beam to draught ratio and the oscillation frequency is given in Diagram 7 of the report by Papanikolaou [10]. Again, the values for zero oscillating frequency should be used. Similar to m_{yy}', these values will be approximated in this study using the following function:

$$m_{\phi\phi}'=m_{\phi\phi0}+m_{\phi\phi1}\left(\frac{B}{T}\right)+m_{\phi\phi2}\left(\frac{B}{T}\right)^2+m_{\phi\phi3}\left(\frac{B}{T}\right)^3$$

The coefficients $m_{\phi\phi i}$ are determined by regression analysis, resulting in:

$m_{\phi\phi0}=1.5119 \quad m_{\phi\phi1}=-1.7190 \quad m_{\phi\phi2}=0.5524 \quad m_{\phi\phi3}=-0.0317$

Note again that extrapolation will probably result in unrealistic values. The added mass in φ-direction per unit length for a section with draught T can now be calculated with:

7

$$m_{\phi\phi} = \frac{\pi \rho T^4 \frac{B}{T}}{4} \cdot m'_{\phi\phi}$$

Using $m_{\phi\phi}$, the added mass for roll is found by:

$$M_{\phi\phi} = \int_L m_{\phi\phi} \, dx.$$

4.7 EQUATIONS OF MOTIONS

To calculate the ship-fixed accelerations $\vec{a}$ of the planing ship, the equations of motions are derived from Newton's second law: $M^{-1} \cdot \Sigma F = \vec{a}$:

$$M^{-1} \cdot \begin{bmatrix} X & - & m(qw-rv) \\ Y & - & m(ru-pw) \\ Z & - & m(pv-qu) \\ K & + & (I_{yy}-I_{zz})qr & + & I_{xz}pq \\ M & + & (I_{zz}-I_{xx})pr & - & I_{xz}(p^2-r^2) \\ N & + & (I_{xx}-I_{yy})pq & - & I_{xz}qr \end{bmatrix} = \begin{bmatrix} \dot{u} \\ \dot{v} \\ \dot{w} \\ \dot{p} \\ \dot{q} \\ \dot{r} \end{bmatrix}$$

in which the mass matrix M is:

$$M = \begin{bmatrix} m+M_{xx} & 0 & 0 & 0 & 0 & 0 \\ 0 & m+M_{yy} & 0 & M_{y\phi} & 0 & M_{y\psi} \\ 0 & 0 & m+M_{zz} & 0 & M_{z\theta} & 0 \\ 0 & M_{y\phi} & 0 & I_{xx}+M_{\phi\phi} & 0 & -I_{xz}+M_{\phi\psi} \\ 0 & 0 & M_{z\theta} & 0 & I_{yy}+M_{\theta\theta} & 0 \\ 0 & M_{y\psi} & 0 & -I_{xz}+M_{\phi\psi} & 0 & I_{zz}+M_{\psi\psi} \end{bmatrix}$$

Solving the above equation at each time step will give the accelerations. Integration of these accelerations provides the velocities u, v, w, p, q and r, which determine the excitation forces ΣF at the next time step.

Transforming the velocities from the ship-fixed coordinate system to the earth-fixed system and subsequently integrating these earth-fixed velocities will provide the position of the ship in the earth-fixed system.

5. SIMULATIONS

In this section, the simulations performed during the study are described. The simulations were done to ascertain whether the program is working properly to evaluate the results of the computations. First the set-up of the test program is discussed, after which the results of the simulation are given and discussed. Details about the computer program can be found in Reference [18].

5.1 TEST PROGRAM

The test program consists of various types of simulation runs. The following types can be defined:

1. Change in model set-up, e.g. change of mass or position of CG.

2. Change in initial position or velocity, e.g. change of rise or speed.

3. Change in hydrodynamic coefficients, i.e. damping factors and deviation from equilibrium position.

4. Change in manoeuvring mode, e.g. turning circle test and zig-zag test.

The first type is used to determine the trends in the results due to changes in the input. The outcome of some changes can be predicted using general theory or publications about this subject.

The second type is used to determine the ability of the ship to return to its equilibrium position, irrespective of the initial deviation from this equilibrium.

The third type is used for stability criteria, concerning the values of these coefficients.

The fourth type is used to determine the manoeuvrability of the planing ship and the behaviour of the ship during these manoeuvres. Combining the third and fourth types can yield more strict limits than those found using the simulations from type three.

Before starting the test program, a few runs were done with both ship models to determine the values of the damping factors κ_ϕ and κ_θ. A value of $\kappa_\theta = 0.6$ was found to be satisfactorily for both Model 233 and Model 277. The value of κ_ϕ was for Model 233: $\kappa_\phi = 0.6$ and for Model 277: $\kappa_\phi = 0.55$. It appears that Model 277 is less sensitive to roll velocities than Model 233. This will be examined in more detail further on in this paper.

The first run for both models is derived from model experiments performed by Keuning [8], (Model 232-A is Model 233 in this study), and [7], (Model 188 is Model 277 in this study). The following conditions were selected:

	Weight	U	θ_{exp}	θ_{sim}	Rise z_{exp}	Rise z_{sim}
Model 233	164 N	2.3 ms-1	3.7°	3.7°	-4.5 mm	-3.1 mm
Model 277	159.9 N	2.4 ms-1	2.3°	1.5°	-5.3 mm	-3.9 mm

It appears that the mathematical model describes the state of Model 233 rather satisfactorily. For Model 277, the similarity between the test result and the simulation result is less clear. The difference may be caused by differences between the model test set-up and the mathematical model. Such differences exist for example in the set-up of the propulsion and the modelling of the rudder forces.

5.2   SIMULATION RESULTS

In this section the results of some simulation runs will be presented. For the set of runs where the model set-up was changed, the results stated in Table 1 were found.

TABLE 1   Results of first set of simulations

Run ID	Description	Expected behaviour	Simulation result
R233-12	Shift LCG aft	Increase θ	$\theta = 3.72° \to \theta = 4.30°$
R233-13	Shift LCG forward	Decrease θ	$\theta = 3.72° \to \theta = 3.22°$
R233-14	Decrease GM	Increase θ	$\theta = 3.72° \to \theta = 3.73°$
R233-15	Increase GM	Decrease θ	$\theta = 3.72° \to \theta = 3.71°$
R233-16	Decrease mass	Decrease draught	$T = 0.088m \to T = 0.082m$
R233-17	Increase mass	Increase draught	$T = 0.088m \to T = 0.093m$
R277-12	Shift LCG aft	Increase θ	$\theta = 1.49° \to \theta = 2.02°$
R277-13	Shift LCG forward	Decrease θ	$\theta = 1.49° \to \theta = 1.02°$
R277-14	Decrease GM	Increase θ	$\theta = 1.49° \to \theta = 1.50°$
R277-15	Increase GM	Decrease θ	$\theta = 1.49° \to \theta = 1.49°$
R277-16	Decrease mass	Decrease draught	$T = 0.085m \to T = 0.079m$
R277-17	Increase mass	Increase draught	$T = 0.085m \to z = 0.090m$

For all simulations, it appears that the behaviour of the computer program to changes in model set-up is consistent with theory or experience. Also, both ship models respond similarly to the changes in model set-up. However, although the damping factor κ_θ is larger for Model 233 than for Model 277, the oscillations around the equilibrium after the initial disturbance are more pronounced for Model 233.

In the graphs taken from the results of runs R233-13 and R277-13, see Figure 3, the difference in oscillation amplitude and duration can be seen. This can be explained by examining the mathematical model for the pitch moment M, see Reference [15] for more details. The spring term to calculate the damping moment is much larger for Model 277 than for Model 233. For Model 277, any pitch angular velocity will be damped stronger in comparison to Model 233. Because the damping is still unknown it is not possible to draw any conclusions on the difference in behaviour between the to hull forms.

Table 2 was constructed after simulation of the runs, with deviations from the initial equilibrium state. At the end of each simulation, the state of the ship model was returned to the equilibrium state, i.e. sailing at straight course and constant speed. It can therefore be concluded that for the used input the state of the planing vessel is stable. From runs R233-24 and R277-24, it also appears that the vessel is course stable.

In Figure 4 the results of the vertical position of the centre of gravity during runs R233-23 and R277-23 are presented in graphical form. Clearly, the oscillations due to the zero initial vertical (ship-fixed) velocity are larger for Model 233 than for Model 277. However, the vertical velocity in the equilibrium state is also much higher for Model 233 than for Model 277. Examining the results, it is seen that the vertical oscillations are a result of the combined heave-pitch system.

In Table 3, the results of the third set of runs are listed. It is clearly seen that decreasing the damping factors largely affects the stability of the ship. The limit values of the damping factors κ_ϕ and κ_θ below which the behaviour of the ship becomes unstable are probably as follows:

Model 233: $0.15 < \kappa_\phi < 0.30$, $0.15 < \kappa_\theta < 0.30$

Model 277: $0.1375 < \kappa_\phi < 0.275$, $\kappa_\theta < 0.15$

In future studies, the limits for the damping factors can be determined more accurately.

As an example of the behaviour of the model at low damping factors, the results of runs R233-34 and R233-36 are included in Figure 6. The unstable behaviour when the damping factor for roll is decreased is clearly visible in the increasing oscillation amplitudes of the roll angle and the increasing immersion.

TABLE 2 Results of second set of simulations

Run ID	Initial deviation	Simulation result
R233-21	Decrease of speed	$u_{t=0} = 1.285\ ms^{-1} \rightarrow u_{t\infty} = 2.285\ ms^{-1}$
R233-22	Increase of speed	$u_{t=0} = 3.285\ ms^{-1} \rightarrow u_{t\infty} = 2.285\ ms^{-1}$
R233-23	Zero vertical speed	$w_{t=0} = 0.000\ ms^{-1} \rightarrow w_{t\infty} = 0.149\ ms^{-1}$
R233-24	Initial drift $\beta = -5°$	$v_{t=0} = 0.200\ ms^{-1} \rightarrow v_{t\infty} = 0.000\ ms^{-1}$
R233-25	Draught $T - 5\ mm$	$T_{t=0} = 0.0827\ m \rightarrow T_{t\infty} = 0.0877\ m$
R233-26	Draught $T + 5\ mm$	$T_{t=0} = 0.0927\ m \rightarrow T_{t\infty} = 0.0877\ m$
R277-21	Decrease of speed	$u_{t=0} = 1.370\ ms^{-1} \rightarrow u_{t\infty} = 2.370\ ms^{-1}$
R277-22	Increase of speed	$u_{t=0} = 3.370\ ms^{-1} \rightarrow u_{t\infty} = 2.370\ ms^{-1}$
R277-23	Zero vertical speed	$w_{t=0} = 0.000\ ms^{-1} \rightarrow w_{t\infty} = 0.062\ ms^{-1}$
R277-24	Initial drift $\beta = -5°$	$v_{t=0} = 0.207\ ms^{-1} \rightarrow v_{t\infty} = 0.000\ ms^{-1}$
R277-25	Draught $T - 5\ mm$	$T_{t=0} = 0.0796\ m \rightarrow T_{t\infty} = 0.0846\ m$
R277-26	Draught $T + 5\ mm$	$T_{t=0} = 0.0896\ m \rightarrow T_{t\infty} = 0.0846\ m$

TABLE 3 Results of third set of simulations

Run ID	Description	Simulation result
R233-31	Zero pitch angle, $\kappa_\theta = 0.60$	Decreasing oscillations
R233-32	$\kappa_\theta = 0.5\ \kappa_{\theta,0} = 0.30$	Decreasing oscillations
R233-33	$\kappa_\theta = 0.25\ \kappa_{\theta,0} = 0.15$	Increasing oscillations
R233-34	Initial roll angle $\phi = 5°$, $\kappa_\phi = 0.60$	Decreasing oscillations
R233-35	$\kappa_\phi = 0.5\ \kappa_{\phi,0} = 0.30$	Decreasing oscillations
R233-36	$\kappa_\phi = 0.25\ \kappa_{\phi,0} = 0.15$	Increasing oscillations
R233-37	Roll angle $5°$, zero pitch	Decreasing oscillations
R233-38	$\kappa_\phi = 0.5\ \kappa_{\phi,0}, \kappa_\theta = 0.5\ \kappa_{\theta,0}$	Decreasing oscillations
R277-31	Zero pitch angle, $\kappa_\theta = 0.60$	Decreasing oscillations
R277-32	$\kappa_\theta = 0.5\ \kappa_{\theta,0} = 0.30$	Decreasing oscillations
R277-33	$\kappa_\theta = 0.25\ \kappa_{\theta,0} = 0.15$	Decreasing oscillations
R277-34	Initial roll angle $\phi = 5°$, $\kappa_\phi = 0.55$	Decreasing oscillations
R277-35	$\kappa_\phi = 0.5\ \kappa_{\phi,0} = 0.275$	Decreasing oscillations
R277-36	$\kappa_\phi = 0.25\ \kappa_{\phi,0} = 0.1375$	Increasing oscillations
R277-37	Roll angle $5°$, zero pitch	Decreasing oscillations
R277-38	$\kappa_\phi = 0.5\ \kappa_{\phi,0}, \kappa_\theta = 0.5\ \kappa_{\theta,0}$	Decreasing oscillations

TABLE 4 Results of turning circle tests

Run ID	Tactical Diameter	Advance	Transfer	Approach Speed	Speed Loss	Damping Roll	Damping Pitch
	m	m	m	ms^{-1}	%	κ_ϕ	κ_θ
R233-41	11.37	13.50	5.77	2.29	7.6	0.60	0.60
R233-42	11.25	13.62	5.76	2.29	8.5	0.30	0.30
R277-41	12.68	14.45	6.47	2.37	7.1	0.55	0.60
R277-42	12.95	14.66	6.62	2.37	7.3	0.27	0.30
233: Difference	-1.1%	+0.9%	-0.2%	-	+12%	+50%	-50%
277: Difference	+2.1%	+1.5%	+2.3%	-	+2.8%	+50%	-50%
R233-TT	11.37	13.50	5.77	2.29	7.6	0.60	0.60
R277-TT	12.78	14.31	6.48	2.28	7.0	0.55	0.60
Difference	+12.4%	+6.0%	+12.3%	-0.4%	-9.2%	-8.3%	+0%

The simulation results of the turning circle tests for both ship models are summarized in Table 4. The first run of each ship model is with the original damping factor values and with a rudder angle of 35° to starboard. During the second run, the damping factors were divided by two. It should be noted that, except for runs R233-TT and R277-TT, the approach speed of both models is not exactly the same (difference approximately 3.5%), therefore the results are not similar. In these runs, a small influence of the damping factors on the manoeuvring characteristics is seen.

Runs R233-TT and R277-TT were performed to illustrate the difference in manoeuvrability between both ship models. The mass, position of centre of gravity and the approach speed were identical for both ships. In Table 4 and Figure 7 the results of the simulations are included. During the simulations, speed losses of approximately 8% were found, while in reality the speed loss during close turning of planing ships can reach values of 70% or even higher. Implementing rotational velocity dependent hydrodynamic coefficients such as X_{vr} in the mathematical model in the future should increase the accuracy of the simulation program considerably.

TABLE 5   Results of 20/20 zig-zag tests

Run Id	Damping		First overshoot	Second overshoot
	Roll	Pitch	Angle	Angle
R233-43	0.60	0.6	27.3	31.5
R233-44	0.30	0.3	28.9	34.3
R277-43	0.55	0.6	26.5	30.4
R277-44	0.275	0.3	27.1	31.2
233: Difference	-50%	-50%	+5.9%	+8.9%
277: Difference	-50%	-50%	+2.3%	+2.6%

The results from the 20/20 zig-zag tests are stated in Table 5. In this table it is seen that for this manoeuvre Model 233 reacts stronger to changes in the damping factors than Model 277. It appears that decreasing the damping results in an increase of the overshoot angles. In Figure 8 the time samples of both the rudder and yaw angles during run R277-43 are included. Note that a starboard rudder angle has a positive sign in this figure.

6.   CONCLUSION

In this paper, a time-domain computer simulation program to predict the dynamic stability and manoeuvrability of planing ships in still water for six degrees of freedom is described. The formulations used in the program were based on experimental data and additional empirical coefficients taken from literature.

Simulation runs have been performed to ascertain whether the program is working properly and to evaluate the calculation results. Some of these results are discussed in this paper.

Examining the simulations, it is seen that changes in the input of the program resulted in the expected changes in the output. Changing the damping factors appears to have great influence of the behaviour of the ships. Further study should emphasize in determining the dynamic coefficients in the mathematical model more accurately. In general it is concluded that the results from this computer simulation program can be used in the early design stage to predict the stability and manoeuvrability of the planing ship.

7.   ACKNOWLEDGEMENTS

8.   REFERENCES

1.   CLEMENT, E P and BLOUNT, D L: 'Resistance tests of a systematic series of planing hull forms'. SNAME Transactions, Vol. 71, 1963.

2.   HOOFT, J P: Computer simulation of the ship's manoeuvrability, Part 1 & 2. Maritime Research Institute the Netherlands.

3.   HOOFT, J P and NIENHUIS, U: 'The prediction of the ship's manoeuvrability in the design stage'. SNAME Annual Meeting, November 1994.

4.   INOUE, S, HIRANO, M, and KIJIMA, K: 'Hydrodynamic derivatives on ship manoeuvring'. International Shipbuilding Progress, Vol. 28, No. 321, pp. 112-125, 1981.

5.   INOUE, S, HIRANO, M, KIJIMA, K, and TAKASHINA, J: 'A practical calculation method of ship maneuvering motion'.   International Shipbuilding Progress, Vol. 28, No. 325, pp. 207-222, 1981.

6.   KEUNING, J A: Invloed van de Deadrise op het zeegangsgedrag van planerende schepen. Report 794-O Delft University of Technology, June 1988.

7.   KEUNING, J A and GERRITSMA, J: 'Resistance tests of a series of planing hull forms with 25 degrees deadrise angle'. International Shipbuilding Progress, Vol. 29, No. 337, pp. 222-249, 1982.

8. KEUNING, J A, GERRITSMA, J, and VAN TERWISGA, P F: Resistance tests of a series planing hull forms with 30 degrees deadrise angle, and a calculation model based on this and similar series. Report 959, Delft University of Technology, December 1992.

9. LEWANDOWSKI, E M: 'Trajectory predictions for high speed planing craft'. International Shipbuilding Progress, Vol. 41, No. 426, pp. 137-148, 1994.

10. PAPANIKOLAOU, A: 'Hydrodynamische Koeffizienten für die linearen Schwingungen von schwimmenden Zylindern'. Schiffstechnik, Vol. 27, No. 3, pp. 127-166, 1980.

11. PAYNE, P R: 'The vertical impact of a wedge on a fluid'. Ocean Engineering, Vol. 8, No. 4, pp. 421-436, 1981.

12. PAYNE, P R: 'Recent developments in 'added-mass' planing theory'. Ocean Engineering, Vol. 21, No. 3, pp. 257-309, 1994.

13. QUADVLIEG, F F H A: Non linear motions of planing ships. Report 920-S, Delft University of Technology, March 1992.

14. RUTGERSSON, O and OTTOSSON, P: 'Model tests and computer simulations - an effective combination for investigation of broaching phenomena'. SNAME Annual Meeting, New York, N.Y., November 1987.

15. TOXOPEUS, S L: A time domain simulation program for manoeuvring of planing ships. Delft University of Technology, September 1996.

16. TOXOPEUS, S L: Mathematical model of the behaviour of planing ships. Delft University of Technology, August 1996.

17. TOXOPEUS, S L: Model experiments on dynamic stability of planing ships. Delft University of Technology, June 1996.

18. TOXOPEUS, S L: VesSim User's Manual. Maritime Research Institute the Netherlands, to be published.

19. ZARNICK, E E: A nonlinear mathematical model of motions of a planing boat in regular waves. Report DTNSRDC-78/032, David W. Taylor Naval Ship Research and Development Center, March 1978.

20. COHEN, S H, BLOUNT, D L: 'Research Plan for the investigation of Dynamic Instability of small High-Speed Craft', SNAME Transactions, Vol. 94, 1986, pp 197-214.

21. BLOUNT, D L and CODEGA, L T: 'Dynamic Stability of Planing Boats', Marine Technology, Vol. 29, No. 1, January 1992, pp 4-12.
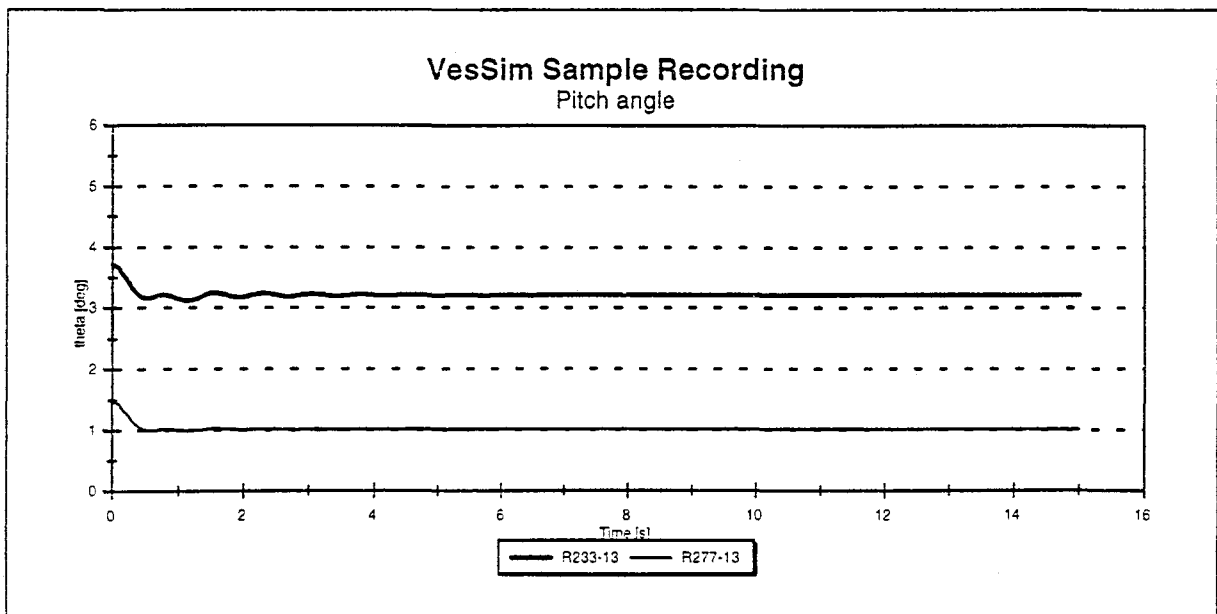
Fig. 3   Results of simulation, runs R233-13 and R277-13

NOMENCLATURE

| Symbol	Description	Unit
C_B	Design block coefficient	-
GM	Metacentric height	m
K	Ship-fixed moment in longitudinal direction	Nm
L	Length between perpendiculars	m
LCG	Longitudinal position centre of gravity	m
$LCOR$	Longitudinal position centre of reference	m
M	Ship-fixed moment in lateral direction	Nm
N	Ship-fixed moment in vertical direction	Nm
p	Rate of turning around x-axis	$rads^{-1}$
q	Rate of turning around y-axis	$rads^{-1}$
r	Rate of turning around z-axis	$rads^{-1}$
T	Draught of the model at centre of reference	m
u	Ship's longitudinal velocity	ms^{-1}
u_e	Ship's longitudinal velocity, earth-fixed	ms^{-1}
U	Towing speed	ms^{-1}
v	Ship's lateral velocity	ms^{-1}
v_e	Ship's lateral velocity, earth-fixed	ms^{-1}
VCG	Vertical position centre of gravity	m
$VCOR$	Vertical position centre of reference	m
w	Ship's vertical velocity	ms^{-1}
X	Ship-fixed force in longitudinal direction	N
x_e	x-position of centre of gravity, earth-fixed	m
x_G	x-position of centre of gravity, ship-fixed	m
x_R	x-position of centre of reference, ship-fixed	m
Y	Ship-fixed force in transversal direction	N
y_e	y-position of centre of gravity, earth-fixed	m
y_G	y-position of centre of gravity, ship-fixed	m
y_R	y-position of centre of reference, ship-fixed	m
z	Rise of centre of reference, coordinate along z-axis	m
Z	Ship-fixed force in vertical direction	N
z_e	z-position of centre of gravity, earth-fixed	m
z_G	z-position of centre of gravity, ship-fixed	m
z_R	z-position of centre of reference, ship-fixed	m
β	Drift angle, twist around earth-fixed z-axis or deadrise angle	deg
θ	Trim angle, twist around ship-fixed y-axis	deg
ϕ	Roll angle, twist around ship-fixed x-axis	deg
ψ	Yaw angle	deg
δ	Rudder angle, positive to port	rad
δ_d	Desired rudder angle	rad
κ_ϕ	Damping factor for roll damping	-
κ_θ	Damping factor for pitch damping	-
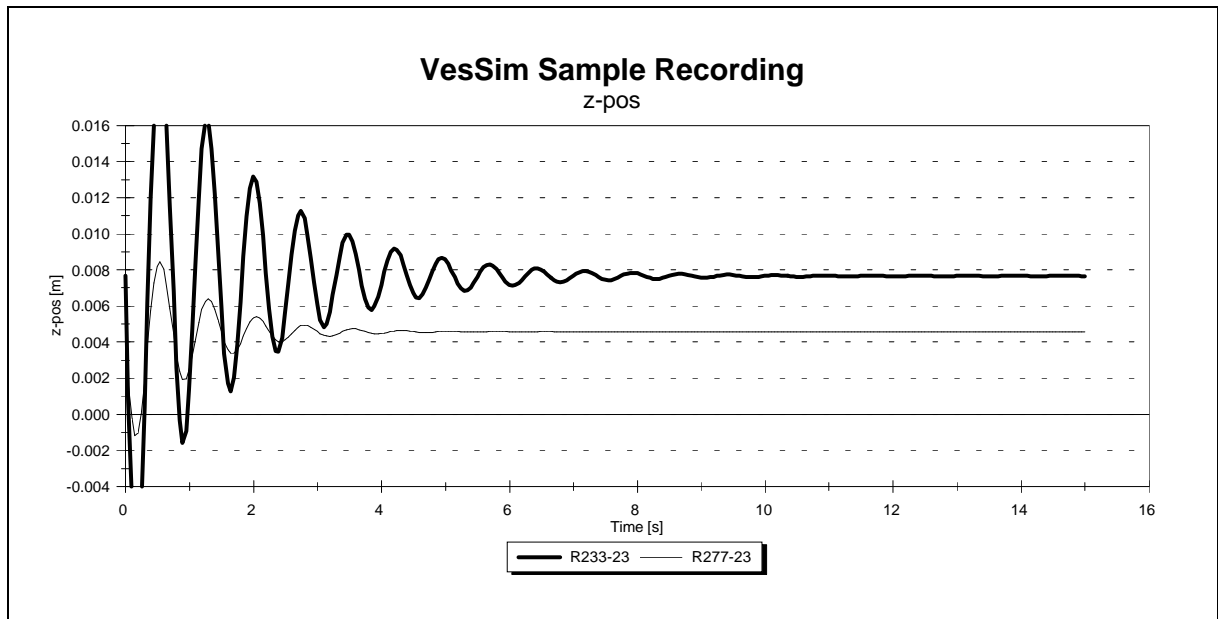
Fig. 4   Results of simulation, runs R233-23 and R277-23
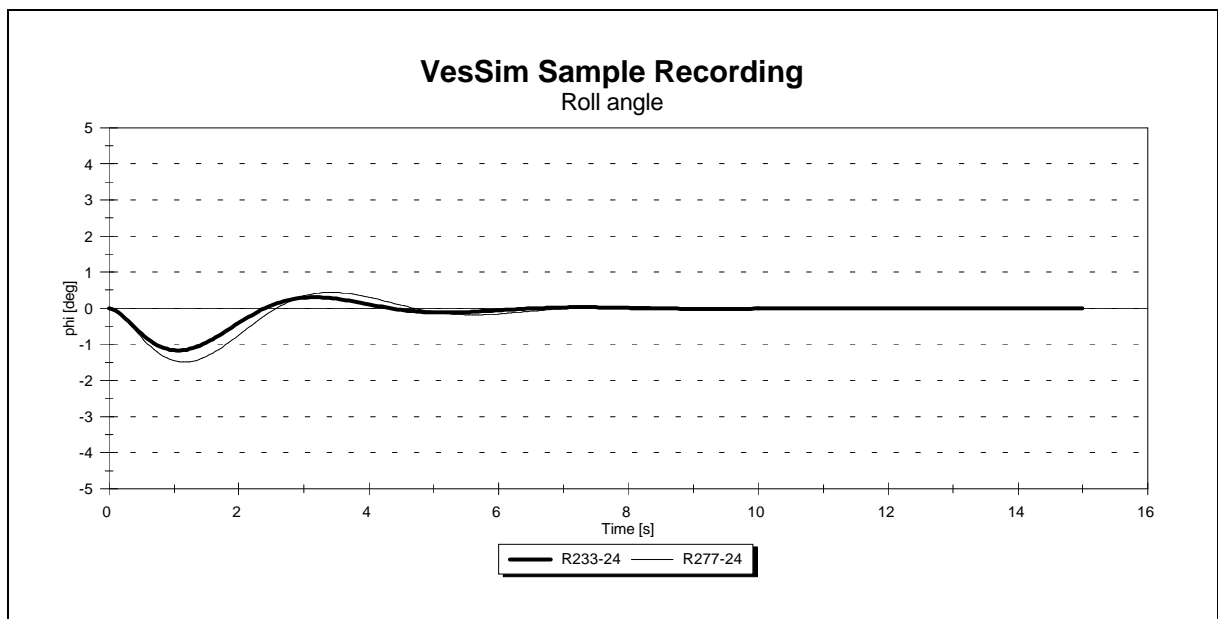

Fig. 5   Results of simulation, runs R233-24 and R277-24
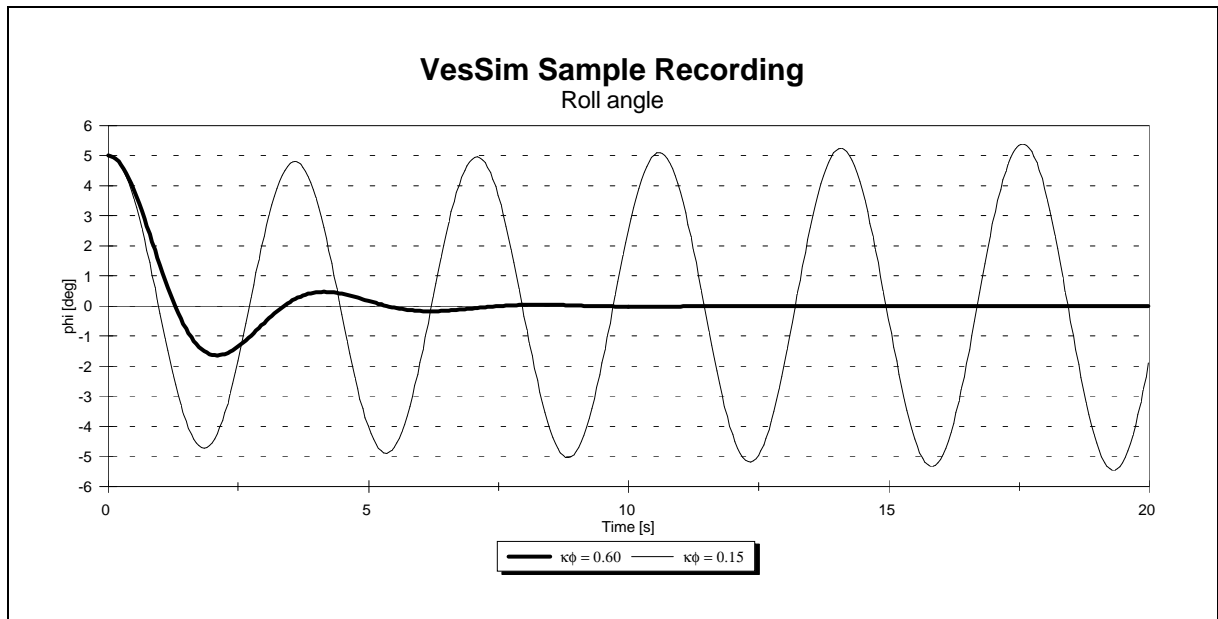
Fig. 6   Results of simulation, runs R233-34 and R277-36
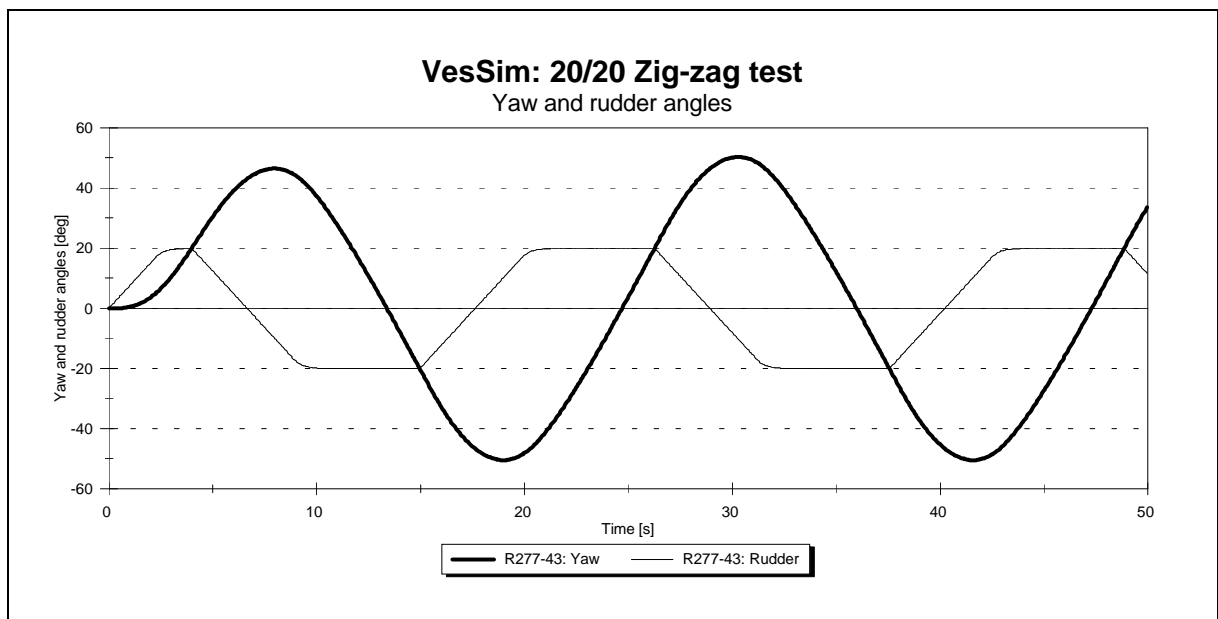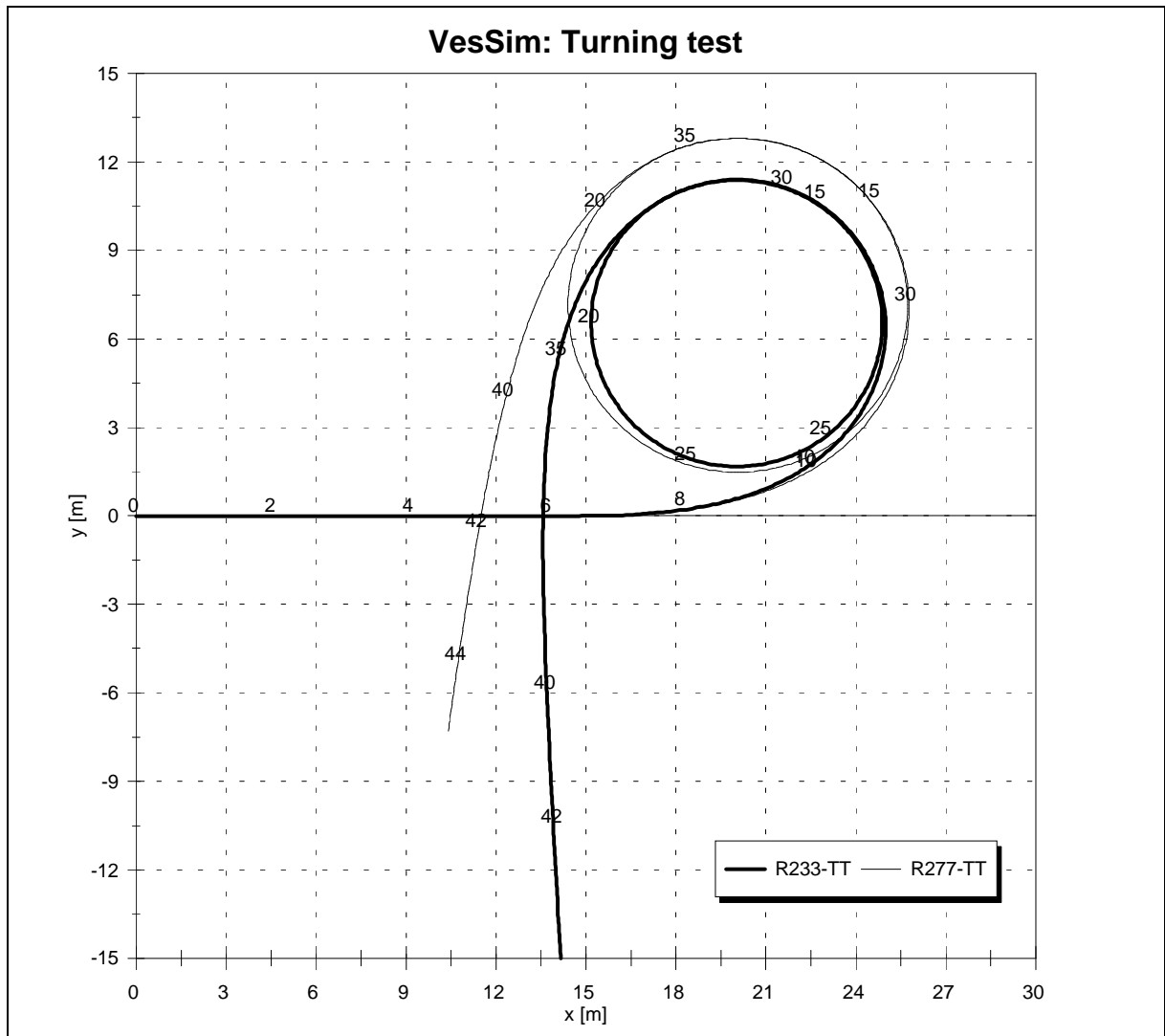

Fig. 8   Results of simulation, run R277-43

Fig. 7 Results of simulation, runs R233-TT and R277-TT